In-vivo and *In-silico* investigation of therapeutic effect of Au-PEG nanoconjugates in Amyotrophic lateral sclerosis (SOD1[G93A])

Sunil Kumar Vimal[1*], Cao Hongyi[1*], Amit Dubey,[2,3] Lokesh Agrarwal,[4] Nishit Pathak[1], Zuo Hua,[1] Deepak Kumar,[5] [1]Sanjib, Bhattacharyya[1#]

[1]Department of Pharmaceutical Sciences, Southwest University, Chongqing 400715, P.R. China.
[2]Computational Chemistry and Drug Discovery Division, Quanta Calculus Pvt. Ltd Kushinagar 274203, India
[3]Department of Pharmacology, Saveetha Dental College and Hospital, Saveetha Institute of Medical and Technical Sciences, Chennai, Tamil Nadu, India.
[4] Molecular Neurobiology group, Okinawa Institute of science and technologies, Japan
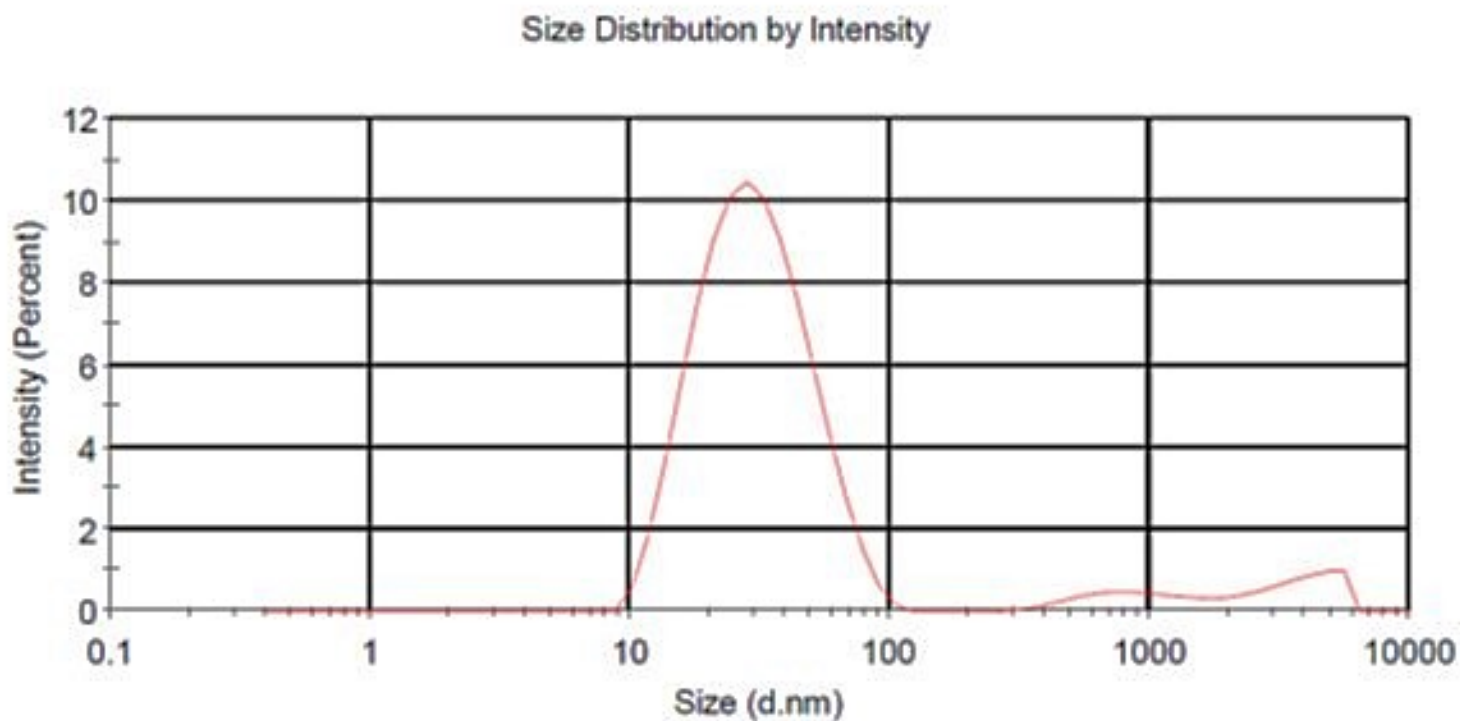[5]Department of Pharmaceutical Chemistry, School of Pharmaceutical Sciences, Shoolini University, Solan, 173229 India


*Equal contribution
Corresponding Author
Sanjib Bhattacharyya (sanjib2017@swu.edu.cn)
Department of Pharmaceutical Sciences and Chinese Traditional Medicine, Southwest University, Beibei, Chongqing, 400715, China

Figure S1: Characterization of size distribution of Au-PEG conjugate using dynamic light scattering (DLS) measurements exhibit the average Au-PEG size 30 nm .
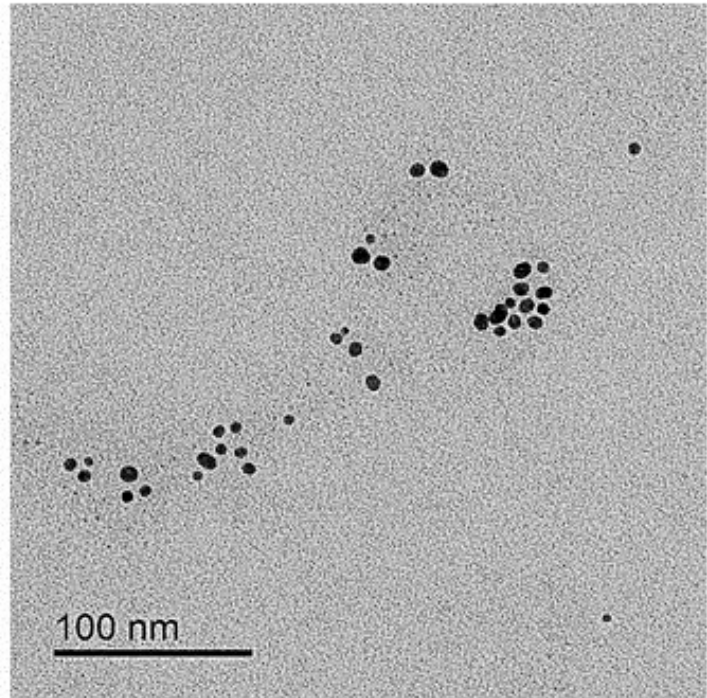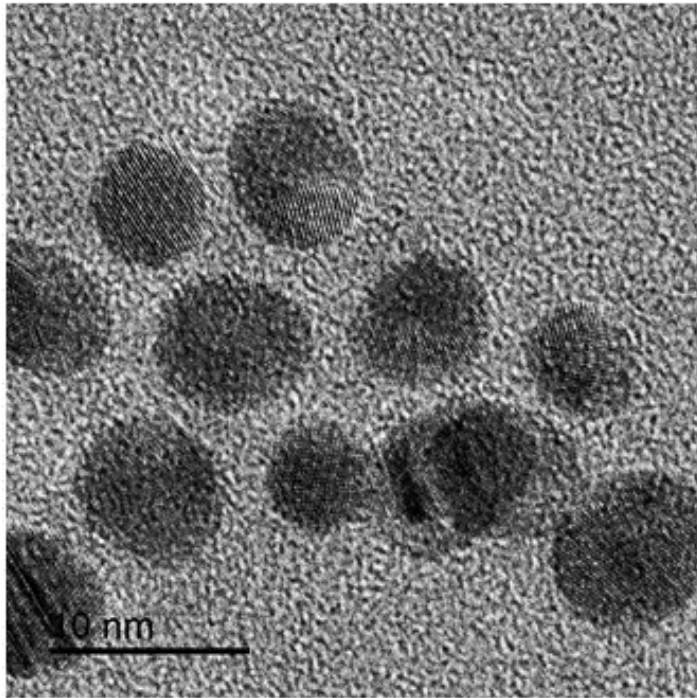
Figure S2: Characterization gold nanoparticles of Au-PEG conjugates using TEM
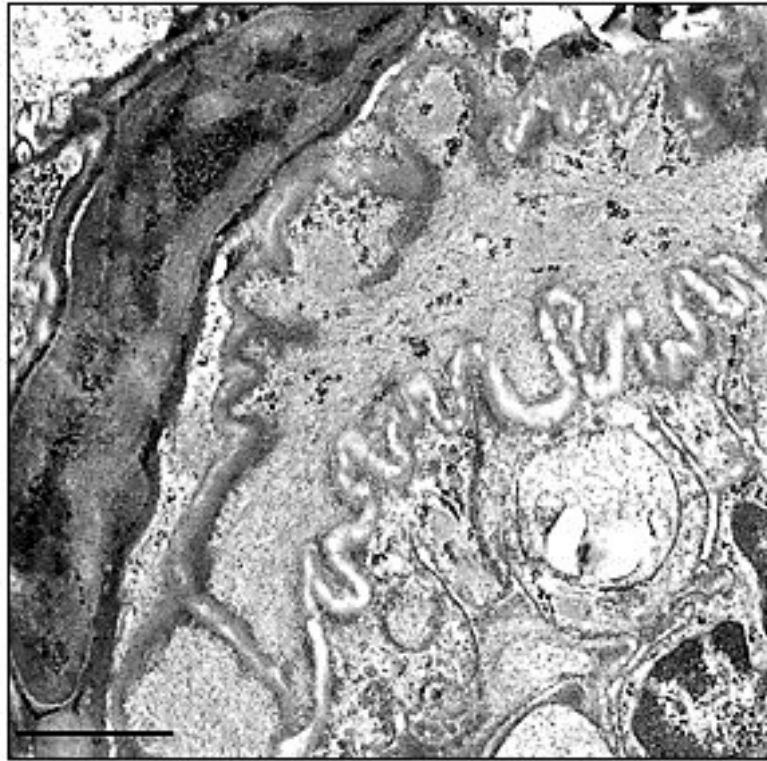
Figure S3: Showing intracellular distribution of Au-PEG. Electron micrographs (TEM) of mice brain section, arrows indicate gold nanoparticle distribution throughout the cellular compartments (Scale bar1 µm).

Figure S4: Pictures are showing key phenotypic symptoms of disease progression in the SOD1-G93A mouse model of ALS. Representative pictures for control mice from a-f) showing body symmetry and hindlimbs abnormality; completely collapsed to rigid paralysis over time. g) loss of control in urination. h-i) less extending in hind limbs. J-k) teary eyes with affected response to object.

Figure S5: Pictures are showing key phenotypic symptoms of disease progression in the SOD1^{G93A} transgenic mouse model of ALS. Representative pictures of Au-PEG treated mice, from a-d) showing body symmetry and hindlimbs abnormality; completely collapsed to rigid paralysis over time. e) loss of control in urination. f) less extending in hind limbs. g-i) teary eyes with affected response to object.
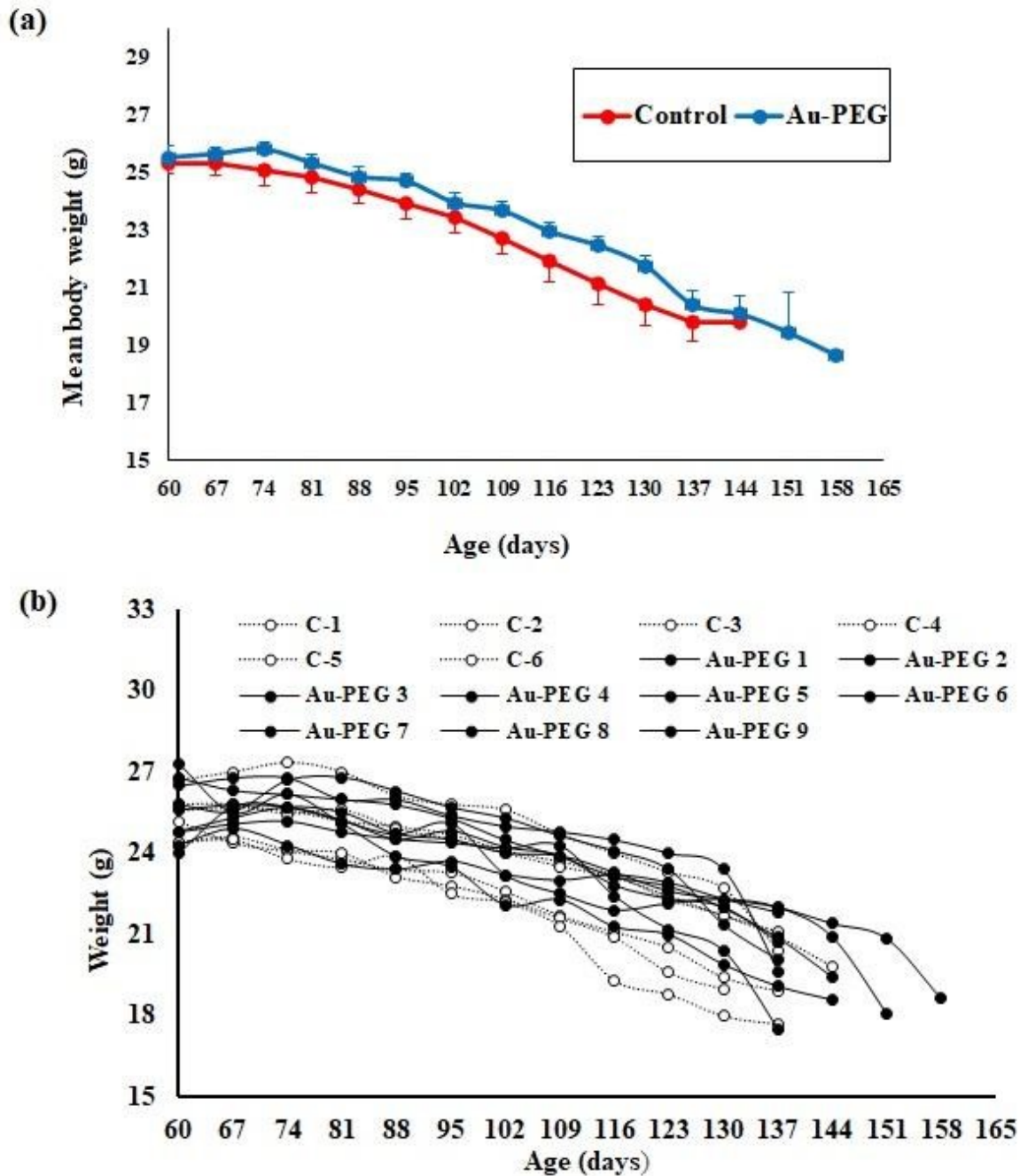
Figure S6: Body weight curves. **(a)** Changes over time in mean body weight of control and Au-PEG treated SOD1^{G93A} transgenic mice (control n=6, treatment n=9). Data are shown as mean ± SEM. No significant differences were noticed between control and treatment group mice. **(b)** Body weight pattern of individual animals   showing during disease progression.
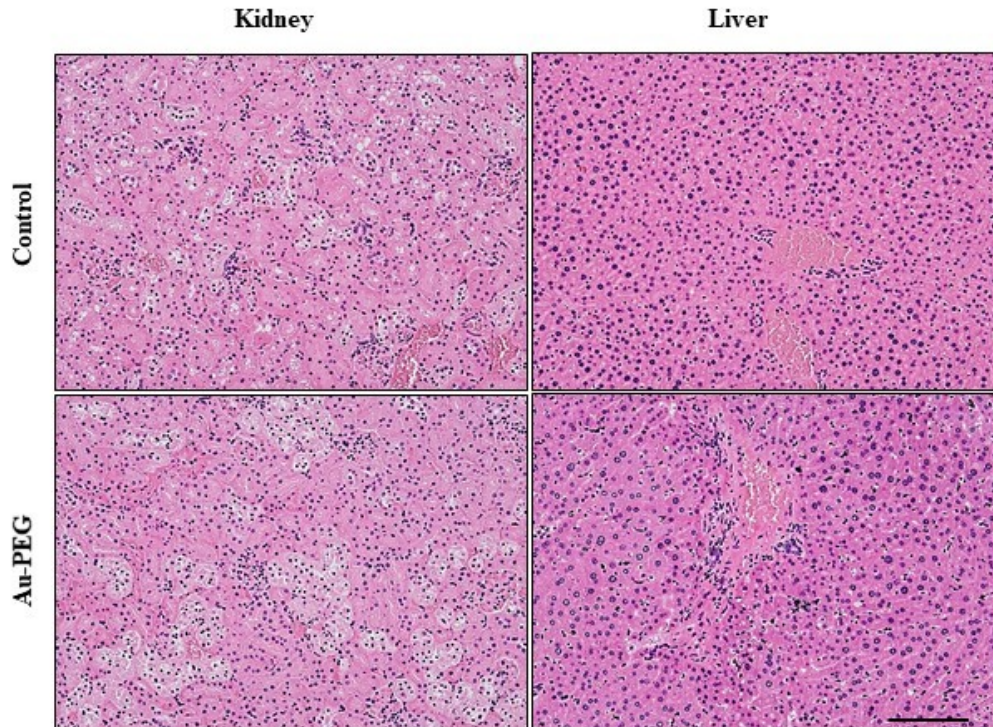
Figure S7: Histological examination of kidney and liver of amyotrophic lateral sclerosis (ALS) in SOD1-G93A mice to assess possible toxic effects of Au-PEG treatment by using hematoxylin/eosin stain. Images were taken at 200X magnification (Scale bar=200μm).
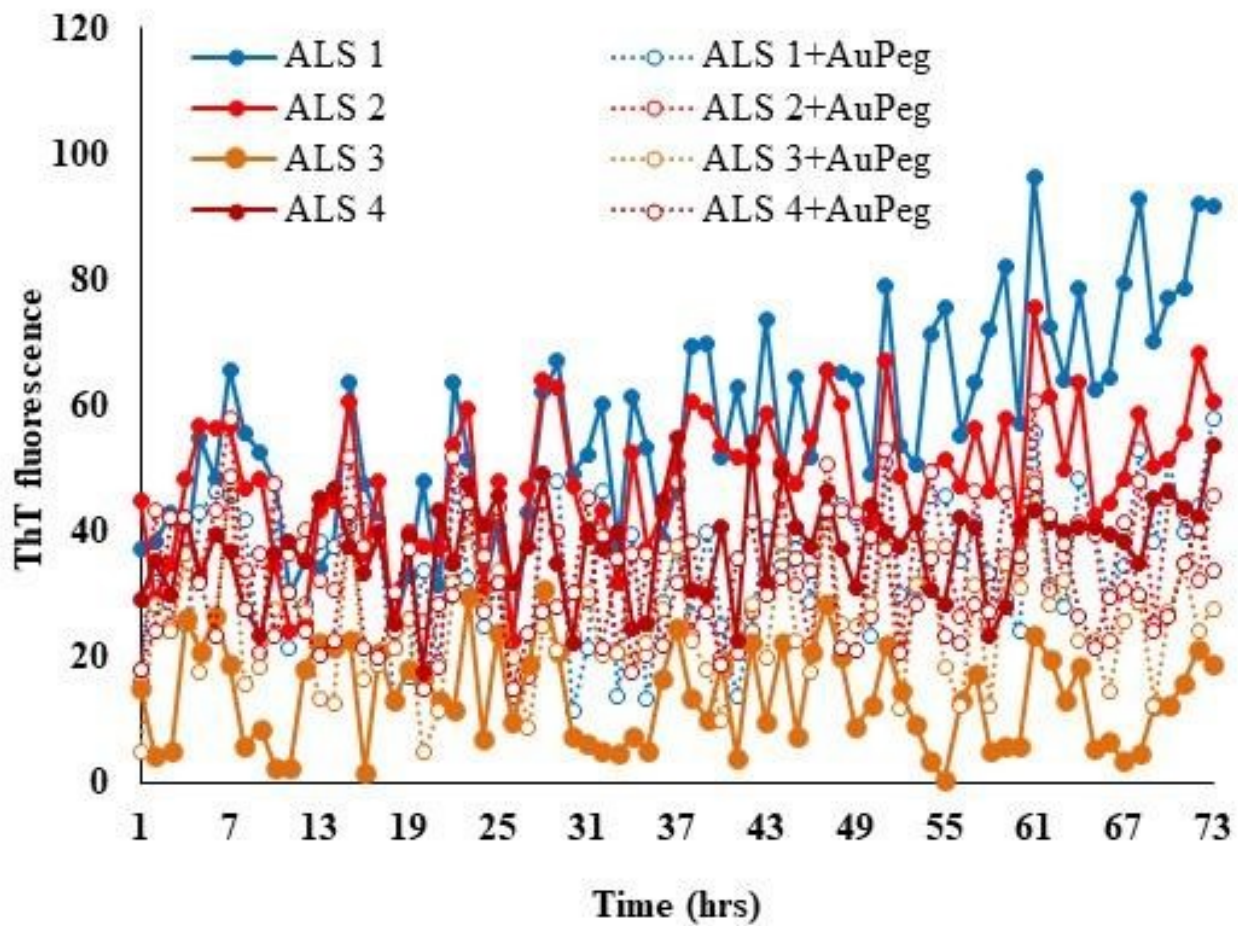
Figure S8: ThT assay showing therapeutic efficacy of Au-PEG against human serum of ALS patient. Serum of ALS Human patient (n=4) incubated with/without Au-PEG using solution of thioflavin T dye (20 μmole) and fluorescence intensity was measured.

Table S1: Human serum of Amyotrophic lateral sclerosis patient

S. No	Hu... Co...					Race
1	BRI					Caucasian
2	BRI					Caucasian
3	BRI					Caucasian
4	BRI					Caucasian

Table S2: Interaction analysis of protein-protein complexes from computational docking

Proteins (PDB Code)	1UXM Residues	6BBN residues	Distance	Interaction type
A4V Human SOD1 (1UXM) + Tubulin (6BBN)	Ser142 (Chain E)	Asn36 (Chain P)	2.6 A^0	Hydrogen Bond, Van der Waals clashes
	Gly130	Arg304	2.6 A^0	Van der Waals clashes (5)
	Gly130	Leu304	2.6 A^0	Van der Waals clashes (5)
G93A Human SOD1 (3GZO) + Tubulin (6BBN)	3GZO Residues			
	Ala93 (Chain C)	Lys338 (Chain C)	2.6 A^0	Hydrogen Bond
	Asp92	Thr337	2.4 A^0	Hydrogen Bond
	Lys23 (Chain A)	Glu100	3.2 A^0	Salt bridge
	Gln153	Leu42	3.3 A^0	Van der Waals clashes
	Pro13	Arg215	2.8 A^0	Van der Waals clashes (5)
	Lys36	Lys299	3.1 A^0	Van der Waals clashes (5)
	Ala55 (Chain H)	Arg308 (Chain B)	2.4 A^0	Van der Waals clashes
	Thr54	His309	2.1 A^0	Van der Waals clashes (5)
	Thr54	Tyr342	2.7 A^0	Van der Waals clashes (2)
	Leu42 (Chain C)	Ala55 (Chain G)	3.3 A^0	Van der Waals clashes
	Lys75	Asp52	2.9 A^0	Salt bridge
	Asp76	Gln153	3.2 A^0	Van der Waals clashes
	Lys91	Val440	2.6 A^0	Van der Waals clashes (2)
	Lys122	Glu40	3.7 A^0	Salt bridge
	Asp76	Lys75	3.0 A^0	Salt bridge

Complex	Hydrophobic	Polar	Negative	Positive	Glycine	Metal
A4V Human SOD1 (1UXM) + Tubulin (6BBN) +Gold	1UXM (Chain E): Ile518 1UXM (Chain L): Pro62, Pro66, Leu67 6BBN (Chain E): Pro500 6BBN (Chain P): Trp112 Phe145	1UXM (Chain L): His63, Asn65, Ser68, His71, His80, Thr135 6BBN (Chain D): Ser423, Asn426, Ser430 6BBN (Chain E): Gln392, Asn498, His501, Thr502, Asn521 6BBN (Chain P): Thr111	1UXM (Chain L): Glu49, Glu77, Glu78, , Asp109, Glu132 6BBN (Chain D): Asp427 6BBN (Chain E): Glu388, Glu520 6BBN (Chain P): Asp143	1UXM (Chain L): Arg69 (Two Salt Bridge), Lys70 (Three Salt Bridges), Lys136 6BBN (Chain D): Arg400 (Three Salt Bridges) 6BBN (Chain E): Lys391 (Two Salt Bridge), Lys499, Arg514 (salt Bridge) 6BBN (Chain P): Lys144 (Four Salt Bridges), Lys147 (Two Salt Bridges)	6BBN (Chain E): Gly519 6BBN (Chain P): Gly146	1UXM (Chain H): Mol H: 0 (Five Metal Coordination)
G93A Human SOD1 (3GZO) + Tubulin (6BBN) +Gold	6BBN (Chain B): Phe399, Met416 6BBN (Chain C): Val437, Val440 6BBN (Chain E): Tyr268 3GZO (Chain H): Pro13, Leu38, Leu42, Ala89	3GZO (Chain D): Thr39 3GZO (Chain E): Thr88, Ser142 6BBN (Chain B): Thr419 , Ser423, Asn426 6BBN (Chain C): Ser439 6BBN (Chain E): Gln177, Gln178, Thr266	3GZO (Chain H): Glu40, Asp90, Asp92, Glu121 6BBN (Chain B): Glu415, Glu422 6BBN (Chain C): Asp345, Asp438 6BBN (Chain E): Asp264	6BBN (Chain B): Arg400 (Two Salt Bridges, Arg401 (Salt Bridge), Lys402 (Three Salt Bridges), 6BBN (Chain E): Arg173, Lys262 (Three Salt Bridges) 3GZO (Chain H): Lys91 (Salt Bridge), Lys122 (Two Salt Bridges)	3GZO (Chain H): Gly37, Gly41	3GZO (Chain H): Mol0 (Ten Metal Coordination) Mol H: 0 (Three Metal Coordination)

Table S3: Docking Results showing amino acid residues participated in the interactions with the A4V Human SOD1 complexed with Tubulin with AuNPs and G93A Human SOD1 complexed with Tubulin with AuNPs

A4V Human SOD1- Tubulin with AuNP interaction

To analyze the binding position occupied by the AuNPs in the selected A4V Human SOD1- Tubulin protein docked complexes, initially AuNPs were aligned to the Tubulin Chain D, E and P) (**Figure 3a**). Remarkably, AuNPs showed occupancy in between the binding cavity of A4V Human SOD1-Tubulin with <10 Å RMSD. Furthermore, AuNPs with A4V Human SOD1- Tubulin protein was analyzed for docking energy and molecular contact formation around the ligand at 4 Å distance, including, □-□/□-cation, hydrophobic, polar, negative, positive, and glycine interactions, (**Figure 3b**). A4V Human SOD1- Tubulin with AuNP complex revealed -17.5 kcal/mol docking score via formation of two and three Salt Bridges bonds at A4V SOD1 (Chain L) Positive Residues Arg69

residue and Lys70 residue respectively. Five metal coordination bonds make the AuNPs more stable inside the A4V SOD1 and Tubulin complex. However, Positive residues of Tubulin (Chain D, E and P) involve   an   overall maximum number of Salt Bridges formations at Lys144, Lys147, Lys391, Arg400, Lys499, Arg514 (**Table S3**).

G93A SOD1- Tubulin-AuNPs Interaction

AuNPs occupied the selected binding region between G93A Human SOD1- Tubulin protein docked complexes. Here, AuNPs were aligned to the Tubulin Chain B, C and E) (**Figure 4a**). However, AuNPs also showed occupancy in between the binding cavity of G93A Human SOD1-- Tubulin with <10 Å RMSD. Additionally, AuNPs with G93A Human SOD1- Tubulin protein was investigated for its docking energy and molecular contact formation around the AuNPs at 4 Å distance, including, □-□/□-cation, hydrophobic, polar, negative, positive, and glycine interactions, (**Figure 4b**). G93A Human SOD1- Tubulin with AuNPs complex interpreted with maximum -17.8 kcal/mol docking score and patchdock score 13404 (Table 2 and Table 3) by substantial contribution of one and two Salt Bridges bonds at G93A SOD1 (Chain H) Positive Residues Lys91 and Lys122 respectively. Exceptionally, with maximum metallic bond (Thirteen metal coordination bonds) make the AuNPs more stable in between the G93A SOD1 and Tubulin complex. However, Positive group of amino acids of Tubulin Chain B, residues Arg400, Arg401 and Lys402 involved with Salt bridges formations and Chain E, residues Arg173 and Lys262 makes maximum number of Salt Bridges formations (**Table S3**).

Superposition of A4V Human SOD1- Tubulin over A4V Human SOD1- Tubulin protein complex with AuNPs

The docked complex A4V Human SOD1- Tubulin over docked complex of A4V Human SOD1- Tubulin protein complex with AuNPs were superposed to investigate the sequence and structure similarity in the interaction region. The complexes interacting sites align well, with a C-alpha atoms RMSD of 49.0095 with Maximum Diff = 119.0261 between atoms 3910 & 4152
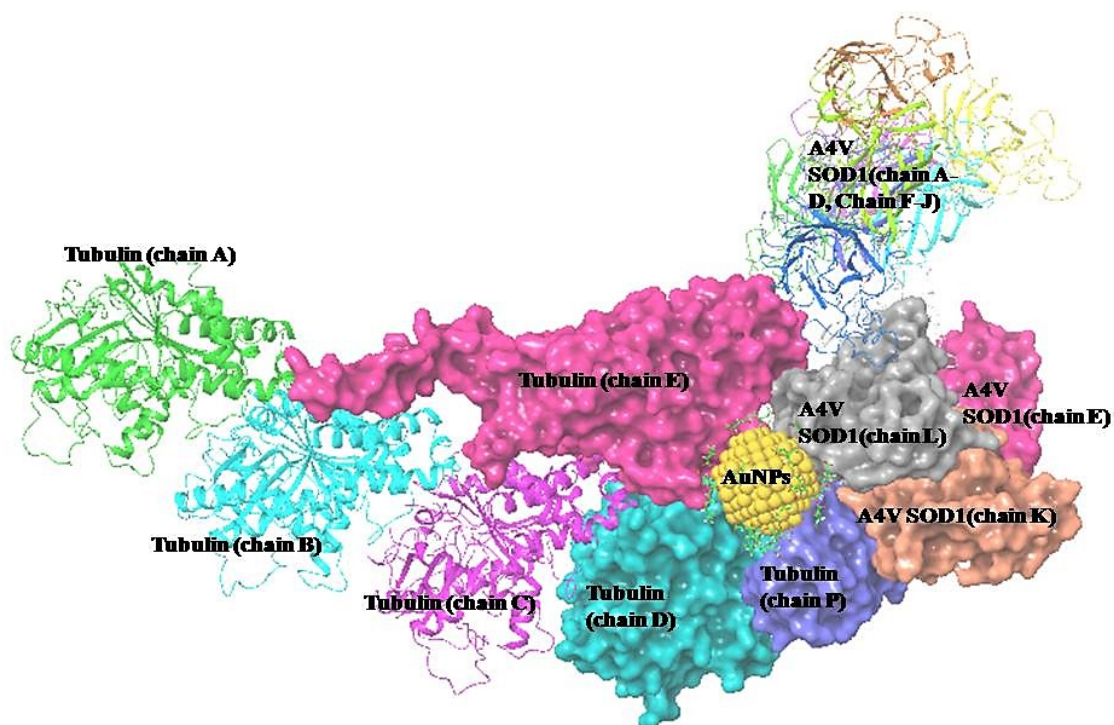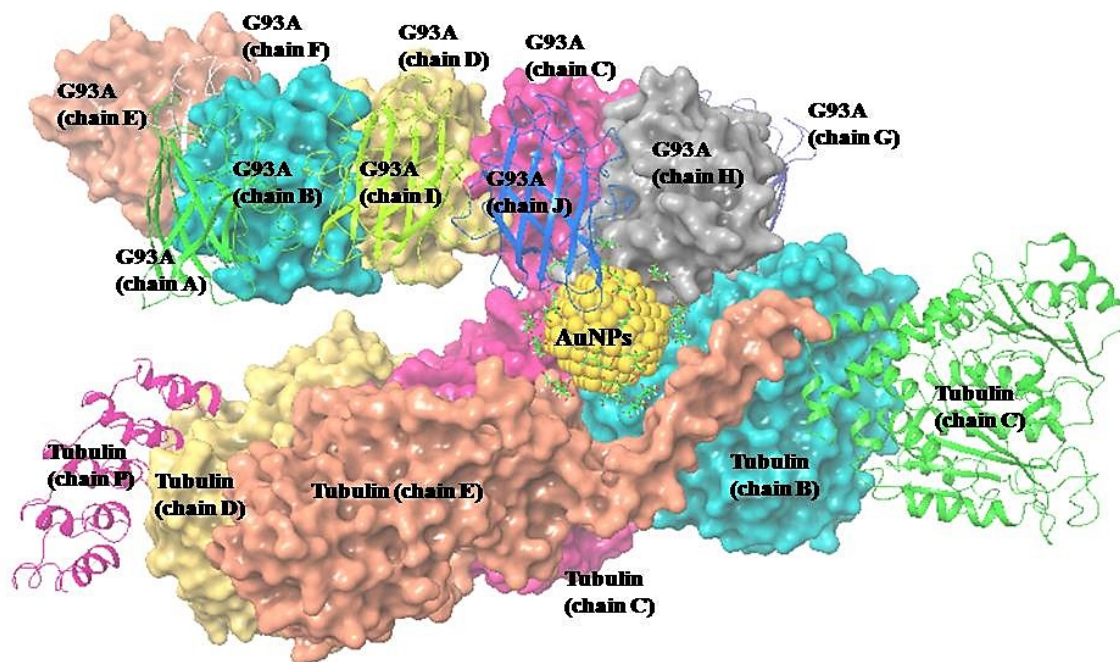
Figure S9: Superimposed overlay of docked complex of A4V Human SOD1- Tubulin protein complex (All Chains) (Ribbon Cartoon Structures) over A4V Human SOD1- Tubulin protein complex with AuNPs (Surface map Structures) models.

Superimposition of G93A Human SOD1- Tubulin over G93A Human SOD1- Tubulin protein complex with AuNPs

The docked complex G93A Human SOD1- Tubulin over the docked complex of G93A Human SOD1- Tubulin protein complex with AuNPs were also superposed to determine the sequence and

structure similarity in the interaction site region. The complexes interacting sites align well, with a C-alpha atoms RMSD of 63.6274 with Maximum Diff = 146.5903 between atoms 950 & 983

Figure S10: Superimposed overlay of docked complex of G93A Human SOD1- Tubulin protein complex (Ribbon Cartoon Structures) over A4V Human SOD1- Tubulin protein complex with AuNP (Surface map Structures) models.